Electronic Supplementary Material (ESI) for Green Chemistry.

Supplementary Information

Mechanism for the selective epimerization of the glucose mannose pair by Mo-based compounds: towards catalyst optimization

Marcos Rellan-Piñeiro, Miquel Garcia-Ratés, Núria López

Institute of Chemical Research of Catalonia, ICIQ, and The Barcelona Institute of Science and Technology, Av. Països Catalans 16, 43007 Tarragona Spain

Figure SI1. Structure of the reaction intermediates in the Glucose → Mannose epimerization reaction catalysed by $H_3PMo_{12}O_{40}$, $H_6P_2Mo_{18}O_{60}$, α-MoO_3 and α-MoO_{3-x}. Same colour code as in Figure 1.

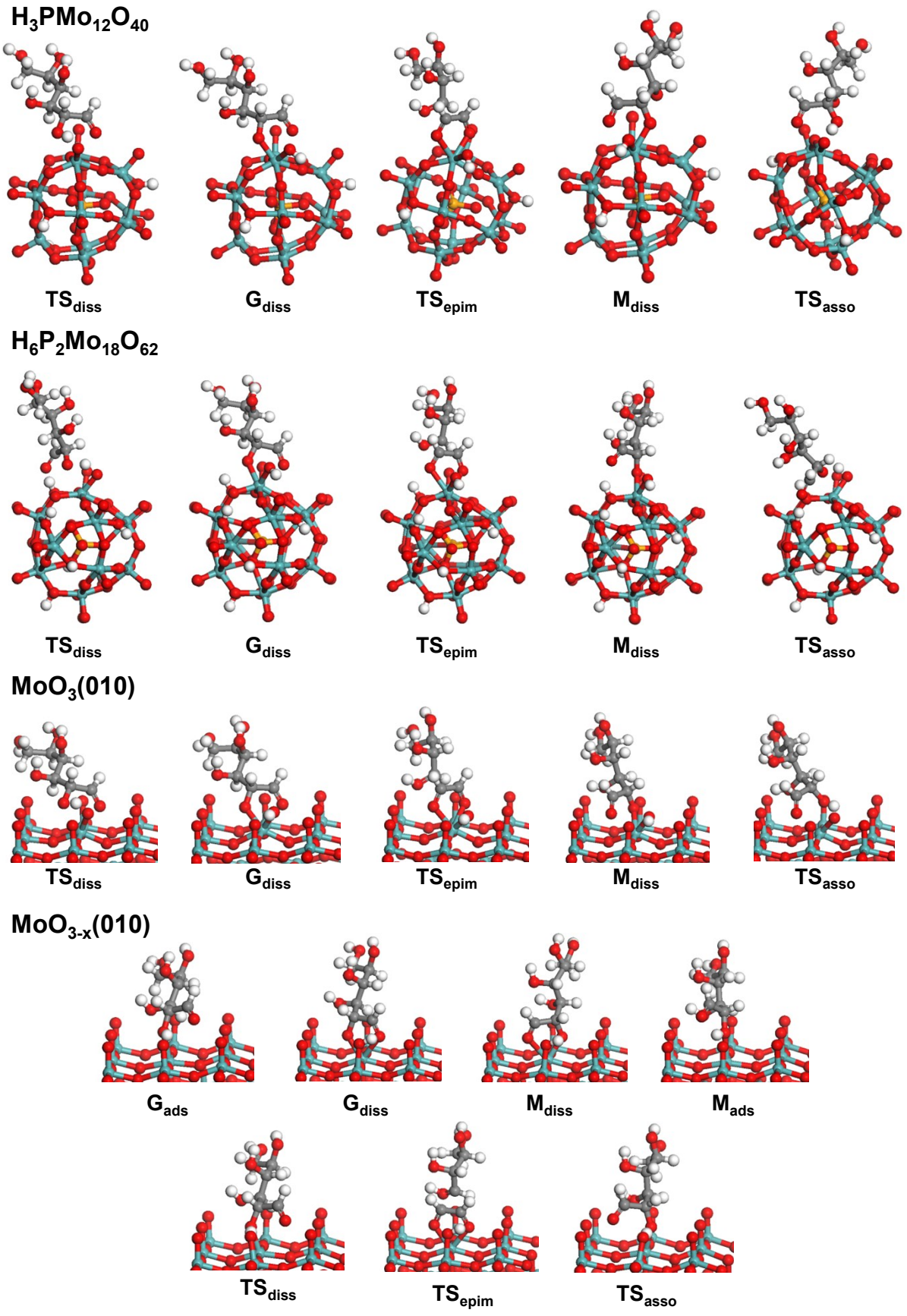

Table SI1. Reaction and activation energy, ΔE and E_a, in eV, for 1,2 C-shift elementary step on $H_3PMo_{12}O_{40}$.

Method/basis	ΔE	$E_{a,1}$	$E_{a,2}$
BP86-D2/set1	-0.04	0.98	1.02
BP86-D2/set2	-0.01	1.07	1.08
PBE-D2/set1	-0.04	0.97	1.01
PBE-D2/set2	-0.03	1.08	1.11
PBE-D2/PW	**-0.02**	**1.03**	**1.05**

set1: 6-311G* for P,O, C, H and LANL2TZ for Mo
set2: 6-311G* for P,O, C, H and TZVP for Mo

Table SI2. Reaction energies, ΔE, energy barriers, E_a (both in eV), and imaginary frequencies, ν_i (cm^{-1}) for all the reaction steps in the Glucose (G) → Mannose (M) epimerization reaction catalysed by $H_3PMo_{12}O_{40}$, $H_6P_2Mo_{18}O_{60}$, α-MoO_3 and α-MoO_{3-x}.

	ΔE	E_a^+	E_a^-	ν_i
$H_3PMo_{12}O_{40}$				
G(g) + * + O* ↔ G* + OH*	0.57	1.04	0.47	828
G* + OH* ↔ M* + OH*	-0.02	0.99	1.01	172
M* + OH* ↔ M(g) + * + O*	-0.64	0.40	1.04	715
$H_6P_2Mo_{18}O_{60}$				
G(g) + * + O* ↔ G* + OH*	0.75	1.07	0.31	739
G* + OH* ↔ M* + OH*	-0.05	1.10	1.15	202
M* + OH* ↔ M(g) + * + O*	-0.79	0.31	1.10	722
α-MoO_3				
G(g) + * + O* ↔ G* + OH*	0.20	1.17	0.97	1036
G* + OH* ↔ M* + OH*	-0.04	0.94	0.98	140
M* + OH* ↔ M(g) + * + O*	-0.24	0.85	1.09	990
α-MoO_{3-x}				
G(g) + * ↔ G*	-1.26	-	-	-
G* + O* ↔ G* + OH*	0.14	0.53	0.39	-
G* + OH* ↔ M* + OH*	-0.04	0.85	0.89	234
M* + OH* ↔ M* + O*	-0.23	0.55	0.78	-
M* ↔ M(g) + *	1.40	-	-	-

Table SI3. Relevant bond distances (Å) for all the reaction intermediates and transition states in the Glucose → Mannose epimerization reaction catalysed by $H_3PMo_{12}O_{40}$, $H_6P_2Mo_{18}O_{60}$, α-MoO_3 and α-MoO_{3-x}.

	Mo-O_1	**Mo-O_2**	**C_1-O_1**	**C_2-O_2**	**C_1-C_2**	**C_1-C_3**	**C_2-C_3**
$H_3PMo_{12}O_{40}$							
TS_{diss}	2.393	2.274	1.237	1.402	1.489	-	1.570
G_{diss}	2.456	1.911	1.230	1.397	1.497	-	1.576
TS_{epim}	2.089	2.137	1.314	1.289	1.407	2.162	2.377
M_{diss}	1.924	2.389	1.400	1.234	1.499	1.576	-
TS_{asso}	2.281	2.477	1.397	1.234	1.500	1.563	-
$H_6P_2Mo_{18}O_{62}$							
TS_{diss}	-	2.279	1.232	1.392	1.499	-	1.580
G_{diss}	2.544	1.922	1.227	1.398	1.504	-	1.565
TS_{epim}	2.109	2.184	1.312	1.236	1.409	2.119	2.268
M_{diss}	1.899	3.297	1.404	1.213	1.533	1.560	-
TS_{asso}	2.229	-	1.398	1.225	1.515	1.581	-
MoO_3							
TS_{diss}	2.475	2.250	1.234	1.420	1.495	-	1.564
G_{diss}	2.385	1.930	1.233	1.412	1.498	-	1.574
TS_{epim}	2.120	2.098	1.303	1.302	1.406	2.222	2.317
M_{diss}	1.919	2.453	1.397	1.231	1.509	1.554	-
TS_{asso}	2.296	2.317	1.403	1.237	1.500	1.556	-
MoO_{3-x}							
G_{ads}	4.079	2.239	1.220	1.444	1.524	-	1.535
TS_{diss}	3.455	1.972	1.219	1.408	1.522	-	1.559
G_{diss}	2.276	1.926	1.239	1.399	1.482	-	1.578
TS_{epim}	2.120	2.046	1.281	1.332	1.397	2.250	2.084
M_{diss}	1.919	2.259	1.398	1.238	1.488	1.567	-
TS_{asso}	1.988	3.605	1.408	1.218	1.526	1.548	-
M_{ads}	4.339	2.204	1.432	1.225	1.526	1.554	-

Figure SI2. Reaction profile, in terms of vibrational Gibbs free energy (Gibbs), for the Bilik reaction for glucose on $H_3PMo_{12}O_{40}$, $H_6P_2Mo_{18}O_{62}$, α-MoO_3(010) and α-MoO_{3-x}(010) at T= 100 ºC.

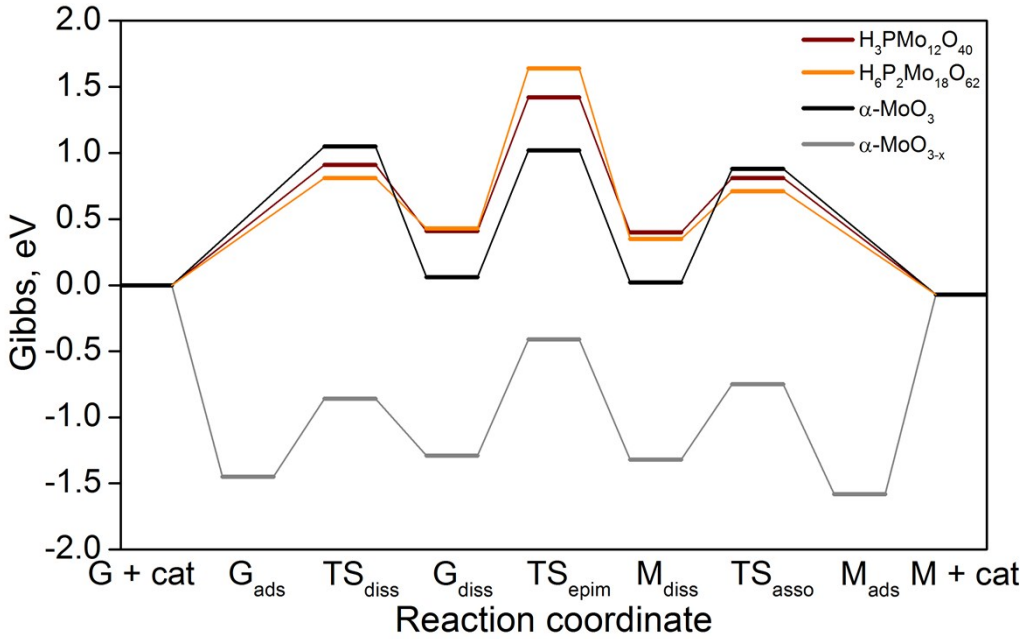

Figure SI3. a) Mechanism scheme for dissociative adsorption of glucose on $H_3PMo_{12}O_{40}$ through $-O^3H$ group. b) Optimized structures for reaction on $H_3PMo_{12}O_{40}$. c) Reaction and activation energies, ΔE and E_a, in eV, for the adsorption of glucose on $H_3PMo_{12}O_{40}$ through $-O^3H$ group.

a)

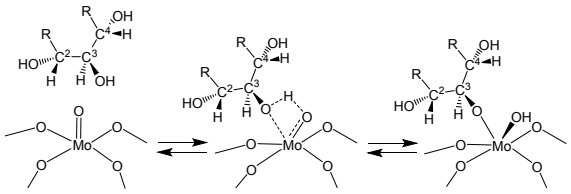

b)

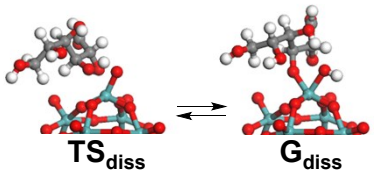

c)

ΔE	E_a^+	E_a^-
0.63	1.01	0.38

Figure SI4. a) Mechanism for the ring opening of glucose and mannose assisted by $H_3PMo_{12}O_{40}$. b) Optimized structures for reaction on $H_3PMo_{12}O_{40}$. c) Reaction profile of the reaction for glucose and mannose on $H_3PMo_{12}O_{40}$.

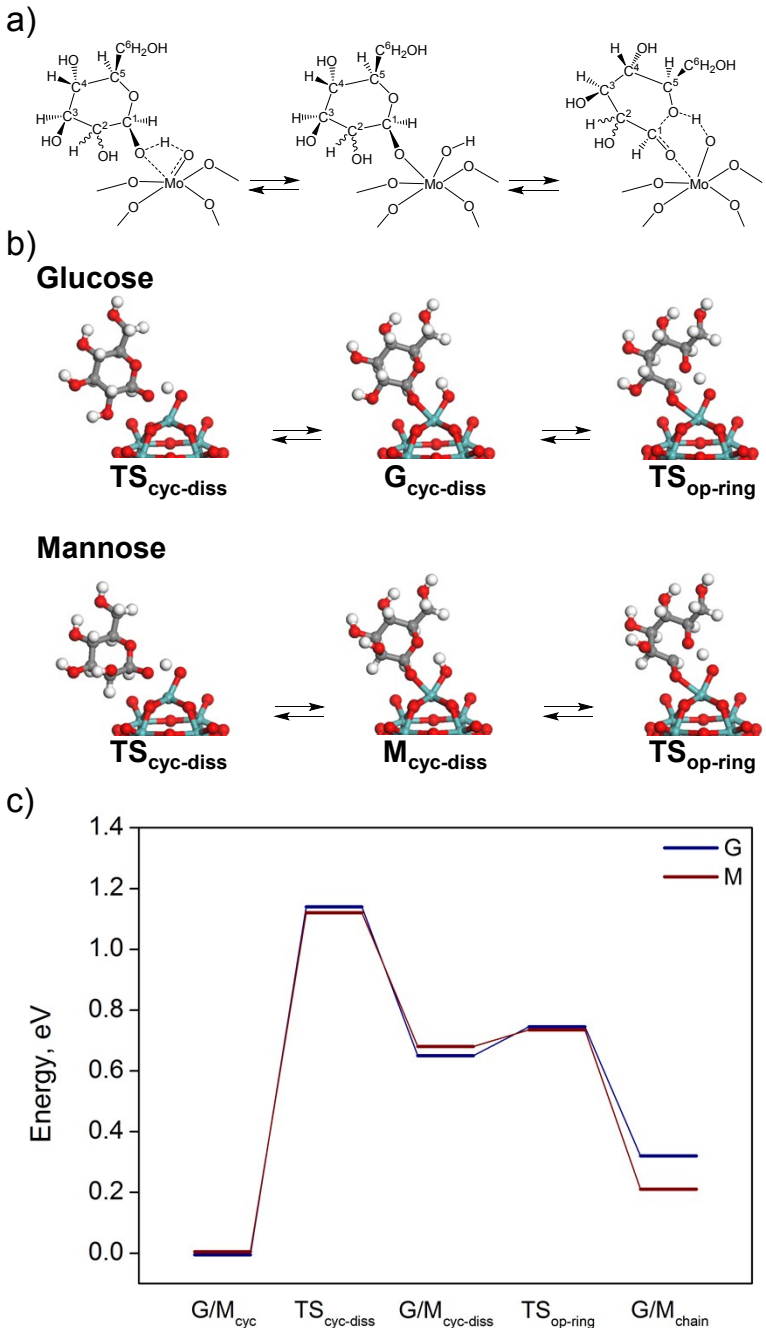

Figure SI5. a) Scheme and converged structures for the dehydration elementary step on the α-MoO_{3-x}(010) surface. b) Reaction path for this step. Energies are given relative to gas-phase glucose and defective surface.

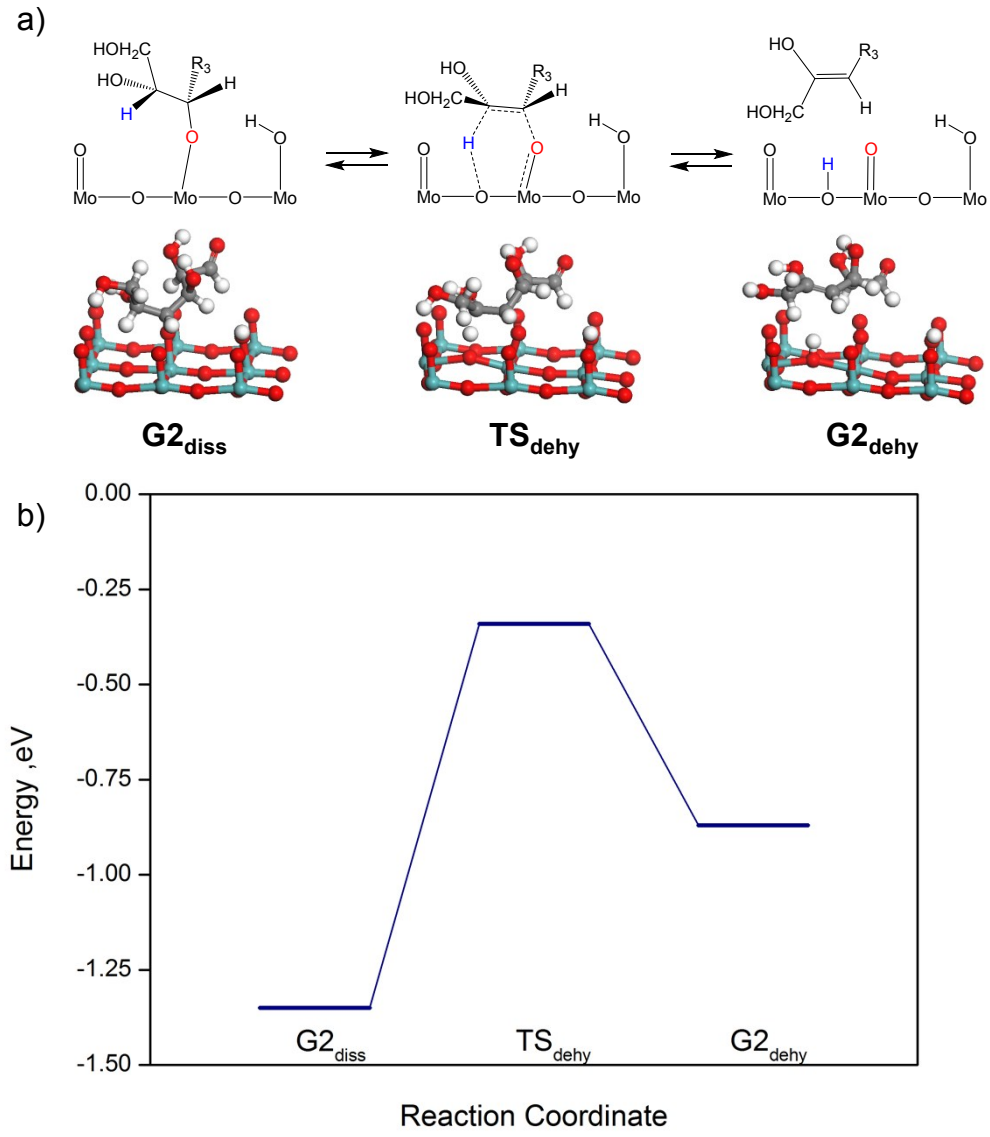

Figure SI6. Energy profile for the epimerization step of glucose to mannose for the case of complete molecules, molecules without $–O_3H$ group and molecules without $–O_4H$ group on $H_3PMo_{12}O_4$.

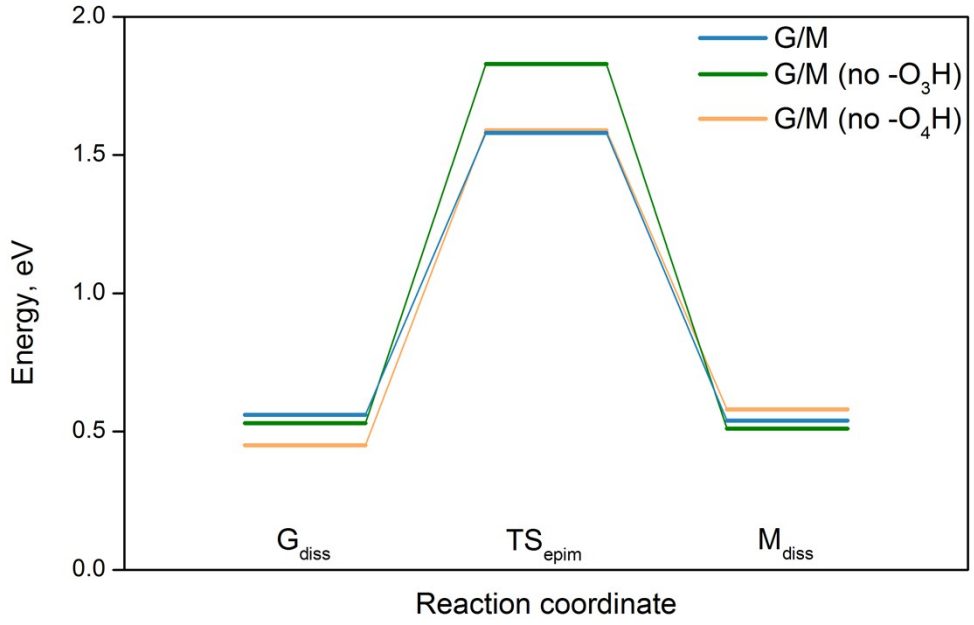

Table SI4. Binding energies, BE, reaction energies, ΔE, energy barriers, E_a, (all in eV) and imaginary frequencies, ν_i (cm^{-1}) for the epimerization step to complete molecules, molecules without $–O_3H$ group and molecules without $–O_4H$ group on $H_3PMo_{12}O_4$.

	BE(G)	**BE(M)**	**ΔE**	**E_a^+**	**E_a^-**	**ν_i**
G/M	0.57	0.55	-0.02	0.99	1.01	172
G/M (no $–O_3H$)	0.55	0.51	-0.04	1.23	1.27	351
G/M (no $–O_4H$)	0.47	0.60	0.12	1.07	0.95	120

Figure SI7. a) Mechanism for the dissociative adsorption of glucose and mannose supported by a water molecule on $H_3PMo_{12}O_{40}$. b) Optimized structures for reaction on $H_3PMo_{12}O_{40}$. c) Reaction profile of the reaction for glucose and mannose on $H_3PMo_{12}O_{40}$.

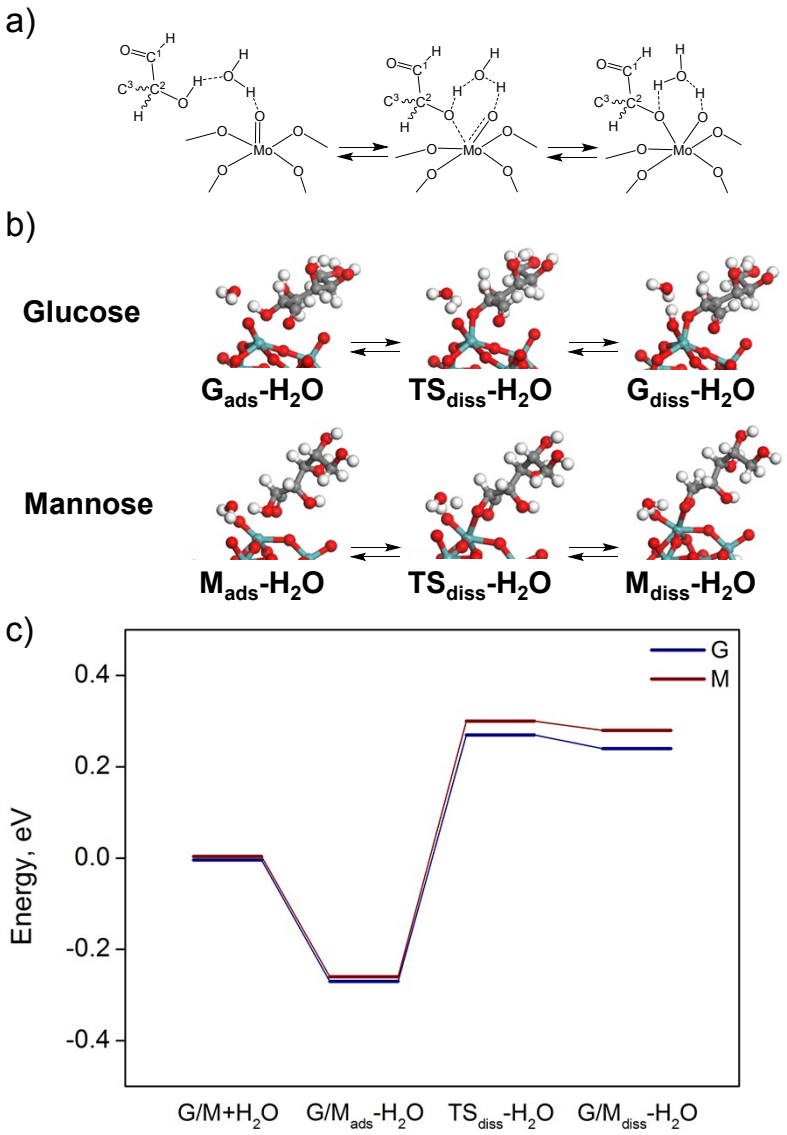

Table SI5. Reaction energies, ΔE, binding energies, BE, and energy barriers, E_a (all in eV), for the 1,2 C-shift step on $H_3PMo_{12}O_{40}$, $[H_2PMo_{12}O_{40}]^-$, $[H_1PMo_{12}O_{40}]^{-2}$, and $[PMo_{12}O_{40}]^{-3}$ in aqueous solution.

	ΔE	**BE(G)**	**BE(M)**	**E_a^+**	**E_a^-**
$H_3PMo_{12}O_{40}$	0.07	0.57	0.64	0.79	0.72
$[H_2PMo_{12}O_{40}]^-$	0.07	0.60	0.67	0.86	0.79
$[H_1PMo_{12}O_{40}]^{-2}$	0.11	0.84	0.95	1.00	0.89
$[PMo_{12}O_{40}]^{-3}$	0.07	1.05	1.12	1.00	0.92

Figure SI8. a) Binding energy, BE, of dissociated glucose and mannose and b) activation energy for the 1,2 C-shift as a function of charge, q in $|e^-|$, on $[H_{n-x}PMo_{12}O_{40}]^{-x}$ (x between 0 and 3). BE(G)= -0.17q + 0.51, R^2= 0.93, MAE= 0.05 eV. BE(M)=-0.17q + 0.57, R^2= 0.93, MAE= 0.04 eV. E_a(G→M)=-0.08q + 0.80, R^2= 0.91, MAE= 0.02 eV. E_a(M→G)= -0.07q + 0.72, R^2= 0.98, MAE= 0.01 eV.

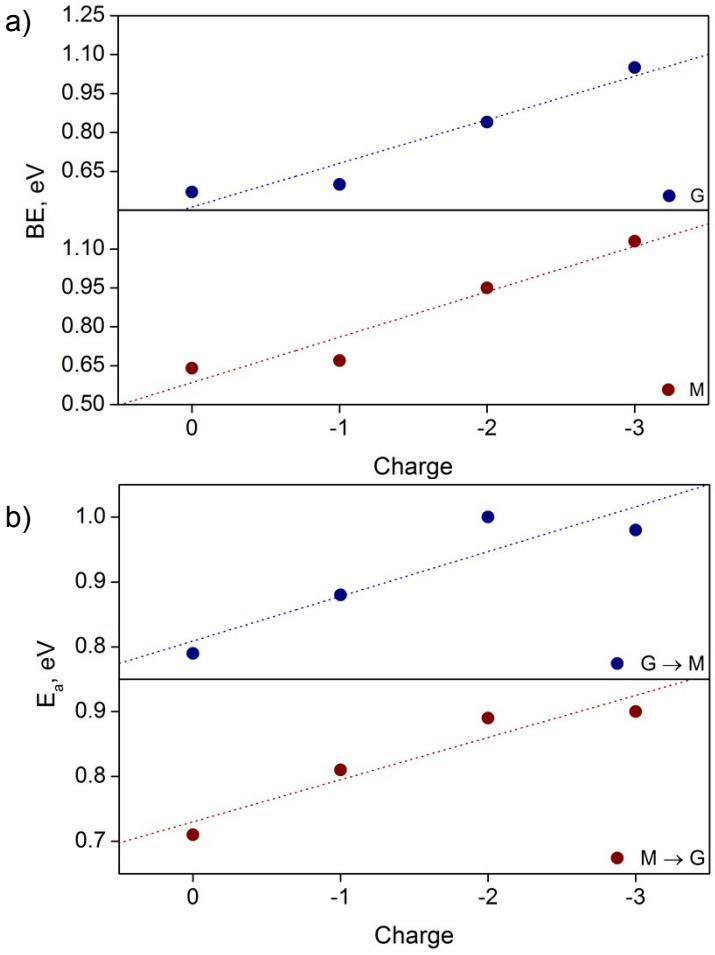

Table SI6. Relevant bond distances (Å) for the intermediates and transition states in Glucose 1,2 C-shift step catalysed by $H_3PMo_{12}O_{40}$, $[H_2PMo_{12}O_{40}]^-$, $[H_1PMo_{12}O_{40}]^{-2}$, and $[PMo_{12}O_{40}]^{-3}$ in aqueous solution.

	Mo-O$_1$	**Mo-O$_2$**	**C$_1$-O$_1$**	**C$_2$-O$_2$**	**C$_1$-C$_2$**	**C$_1$-C$_3$**	**C$_2$-C$_3$**
$H_3PMo_{12}O_{40}$							
G_{diss}	2.362	1.899	1.236	1.411	1.491	-	1.576
TS_{epim}	2.118	2.004	1.302	1.314	1.396	2.634	2.598
M_{diss}	1.903	2.337	1.413	1.240	1.491	1.574	-
$[H_2PMo_{12}O_{40}]^-$							
G_{diss}	2.404	1.920	1.236	1.407	1.493	-	1.576
TS_{epim}	2.150	2.022	1.297	1.319	1.398	2.483	2.354
M_{diss}	1.911	2.384	1.140	1.237	1.495	1.570	-
$[H_1PMo_{12}O_{40}]^{-2}$							
G_{diss}	2.455	1.931	1.233	1.407	1.496	-	1.573
TS_{epim}	2.104	2.133	1.311	1.300	1.400	2.296	2.372
M_{diss}	1.924	2.424	1.406	1.235	1.496	1.569	-
$[PMo_{12}O_{40}]^{-3}$							
G_{diss}	2.828	1.916	1.224	1.402	1.509	-	1.570
TS_{epim}	2.174	2.126	1.297	1.311	1.402	2.302	2.215
M_{diss}	1.937	2.476	1.403	1.233	1.497	1.570	-

Figure SI9. Optimized structures of minima and TS of the 1,2 C-shift assisted by one and two supported water molecules.

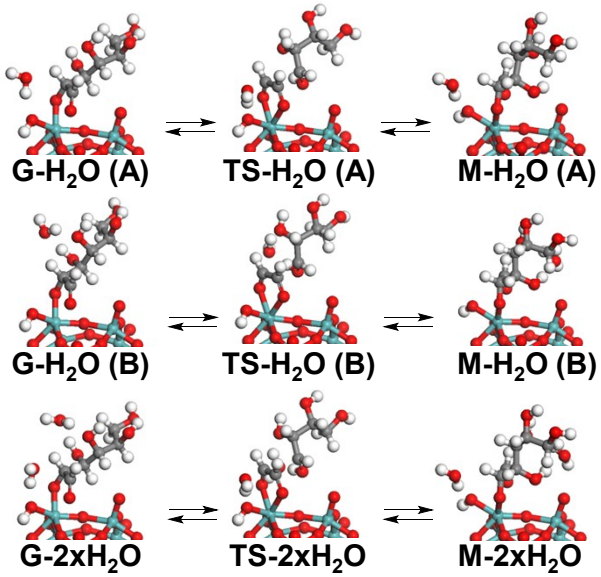

Table SI7. Reaction and activation energy, ΔE and E_a for 1,2 C-shift elementary step on $H_3PMo_{12}O_{40}$, supported by one and two explicit water molecules.

	ΔE	E_a^+	E_a^-
No H_2O	-0.02	1.03	1.05
1xH_2O (A)	0.02	0.91	0.89
1xH_2O (B)	0.07	0.93	0.86
2xH_2O	0.15	0.84	0.70
VASP-MGCM	0.07	0.79	0.72

Figure SI10. Energy profile for the epimerization step of glucose to mannose on $H_nXMo_{12}O_{40}$ (X= S, P, As, Si, Ge).

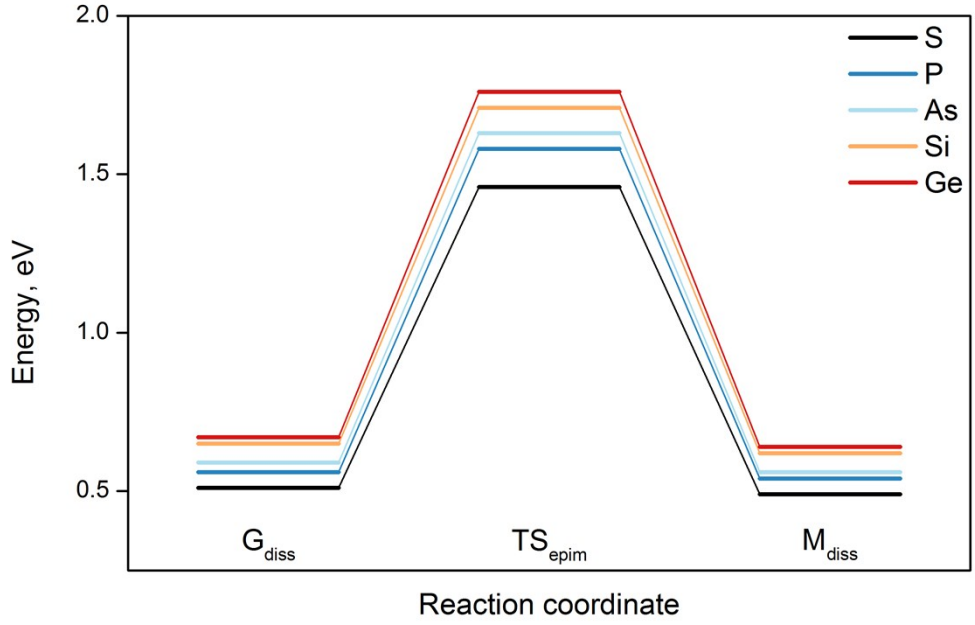

Table SI8. Reaction energies, ΔE, binding energies, BE, (both in eV), and imaginary frequencies, ν_i (cm^{-1}) for the 1,2 C-shift step in Glucose → Mannose epimerization reaction catalysed by $H_nXMo_{12}O_{40}$ (X= S, P, As, Si, Ge).

	ΔE	BE (G)	BE (M)	E_a^+	E_a^-	ν(i)
$H_2SMo_{12}O_{40}$	-0.02	0.51	0.49	0.95	0.97	160
$H_3PMo_{12}O_{40}$	-0.02	0.56	0.54	1.03	1.05	172
$H_3AsMo_{12}O_{40}$	-0.03	0.59	0.56	1.04	1.07	168
$H_4SiMo_{12}O_{40}$	-0.03	0.65	0.62	1.06	1.09	151
$H_4GeMo_{12}O_{40}$	-0.03	0.67	0.64	1.10	1.13	143

Table SI9. Relevant bond distances (Å) for the intermediates and transition states in the 1,2 C-shift step catalysed by $H_nXMo_{12}O_{40}$ (X= P, As, Si, Ge).

	Mo-O_1	**Mo-O_2**	**C_1-O_1**	**C_2-O_2**	**C_1-C_2**	**C_1-C_3**	**C_2-C_3**
$H_2SMo_{12}O_{40}$							
G_{diss}	2.481	1.907	1.229	1.398	1.498	-	1.576
TS_{epim}	2.089	2.137	1.314	1.287	1.407	2.162	2.377
M_{diss}	1.921	2.398	1.399	1.233	1.499	1.576	-
$H_3PMo_{12}O_{40}$							
G_{diss}	2.456	1.911	1.230	1.397	1.497	-	1.576
TS_{epim}	2.089	2.137	1.314	1.289	1.407	2.162	2.377
M_{diss}	1.924	2.389	1.400	1.234	1.499	1.576	-
$H_3AsMo_{12}O_{40}$							
G_{diss}	2.493	1.908	1.229	1.397	1.498	-	1.576
TS_{epim}	2.083	2.149	1.317	1.284	1.408	2.380	2.139
M_{diss}	1.925	2.405	1.399	1.233	1.501	1.575	-
$H_4SiMo_{12}O_{40}$							
G_{diss}	2.517	1.907	1.227	1.397	1.500	-	1.574
TS_{epim}	2.104	2.118	1.306	1.294	1.403	2.344	2.221
M_{diss}	1.923	2.419	1.398	1.231	1.502	1.573	-
$H_4GeMo_{12}O_{40}$							
G_{diss}	2.572	1.905	1.226	1.503	1.396	-	1.575
TS_{epim}	2.108	2.118	1.305	1.295	1.403	2.236	2.339
M_{diss}	1.926	2.427	1.399	1.232	1.503	1.574	-

Table SI10. Bader charges of the atoms of XO_2^{n-} units for $H_nXMo_{12}O_{40}$ (X=S, P, As, Si, Ge).

	X	**O1**	**O2**	**O3**	**O4**	**Total**
$H_2SMo_{12}O_{40}$	3.84	-1.36	-1.36	-1.36	-1.37	-1.61
$H_3PMo_{12}O_{40}$	3.62	-1.45	-1.47	-1.47	-1.47	-2.23
$H_3AsMo_{12}O_{40}$	2.58	-1.19	-1.19	-1.19	-1.19	-2.18
$H_3SiMo_{12}O_{40}$	3.10	-1.45	-1.44	-1.46	-1.47	-2.72
$H_3GeMo_{12}O_{40}$	2.33	-1.26	-1.24	-1.26	-1.27	-2.69

Figure SI11. a) Binding energies, BE, of dissociated glucose and mannose and b) activation energy for the 1,2 C-shift as a function of charge transferred, CT in $|e^-|$, to $H_nXMo_{12}O_{40}$ (X= S, P, As, Si, Ge). BE(G)= -0.17CT + 0.44, R^2= 0.99, MAE= 0.01 eV. BE(M)=-0.13CT + 0.53, R^2= 0.93, MAE= 0.01 eV. E_a(G→M)=-0.11CT + 0.91, R^2= 0.87, MAE= 0.01 eV. E_a(M→G)= -0.14 + 0.90, R^2= 0.95, MAE= 0.03 eV.

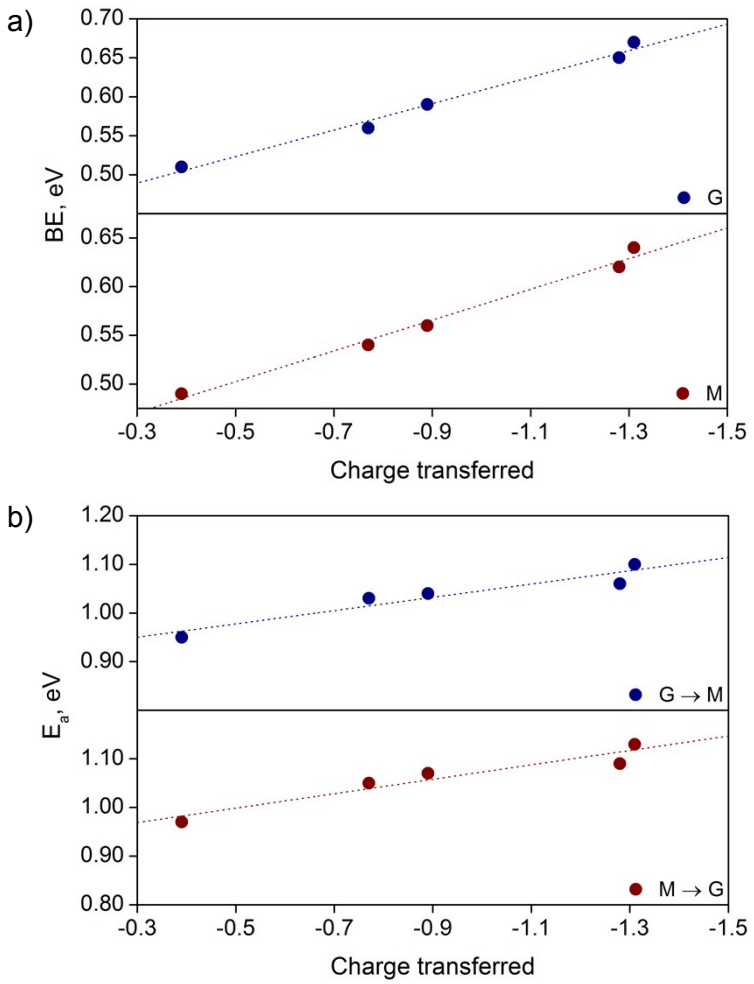

Table SI11. Binding, BE, and activation, E_a, energies, hydrogen addition energy, HAE, Red (all in eV), and Mo-O average bond distances (in Å) for the used catalysts in the linear fitting.

	BE (G)	BE (M)	E_a(G→M)	E_a(M→G)	HAE	Red	r(Mo-O)
$H_2SMo_{12}O_{40}$	0.51	0.58	0.95	0.97	-3.87	-5.86	1.992
$H_3PMo_{12}O_{40}$	0.57	0.64	0.99	1.01	-3.91	-5.82	1.988
$H_3AsMo_{12}O_{40}$	0.61	0.66	1.00	1.03	-3.94	-5.79	1.980
$H_3SiMo_{12}O_{40}$	0.65	0.68	1.02	1.08	-3.95	-5.68	1.983
$H_3GeMo_{12}O_{40}$	0.67	0.71	1.07	1.12	-3.96	-5.66	1.979
$H_6P_2Mo_{18}O_{62}$	0.75	0.79	1.10	1.15	-3.98	-5.50	1.967
α-MoO_3	0.20	0.24	0.94	0.98	-3.79	-	1.992
α-MoO_{3-x}	-1.13	-1.08	0.85	0.89	-3.71	-	2.015

Figure SI12. a) Binding energy, BE, of dissociated glucose and mannose on $H_nXPMo_{12}O_{40}$ (X= S, P, As, Si, Ge) and on $H_6P_2Mo_{18}O_{62}$ and b) activation energy of the 1,2 C-shift as a function of reducibility, Red, of the Mo center. BE(G)= 0.63Red + 4.29, R^2= 0.96, MAE= 0.01 eV. BE(M)=0.54Red +3.76, R^2= 0.93, MAE= 0.02 eV. E_a(G→M)=0.41Red +3.36, R^2= 0.92, MAE= 0.01 eV. E_a(M→G)= 0.51Red +3.99, R^2= 0.94, MAE= 0.01 eV.

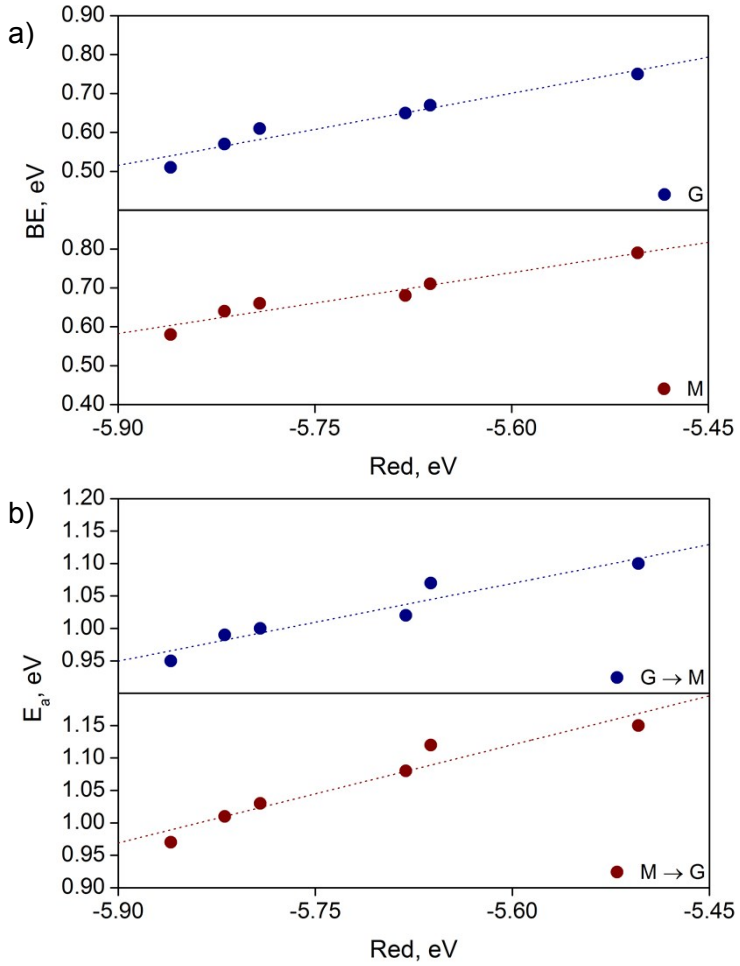

Figure SI13. a) Binding energy, BE, of the dissociated glucose and mannose as a function of the Mo-O average bond distance for the clean catalyst*. BE(G)=-9.03 r_{Mo-O} +18.52, R^2= 0.81, MAE= 0.02 eV. BE(M)=-8.58 r_{Mo-O} +17.58, R^2= 0.90, MAE= 0.04 eV. Adsorption on defective and pristine MoO_3(010) surfaces are not included in the fittings. b) Activation energy, E_a, of TS_{epim} as a function of the Mo-O average bond distance for the clean catalyst. E_a(G→M)=-5.29 r_{Mo-O} +11.53, R^2= 0.92, MAE= 0.02 eV. E_a(M→G)=-5.01 r_{Mo-O} +11.01, R^2= 0.92, MAE= 0.04 eV.

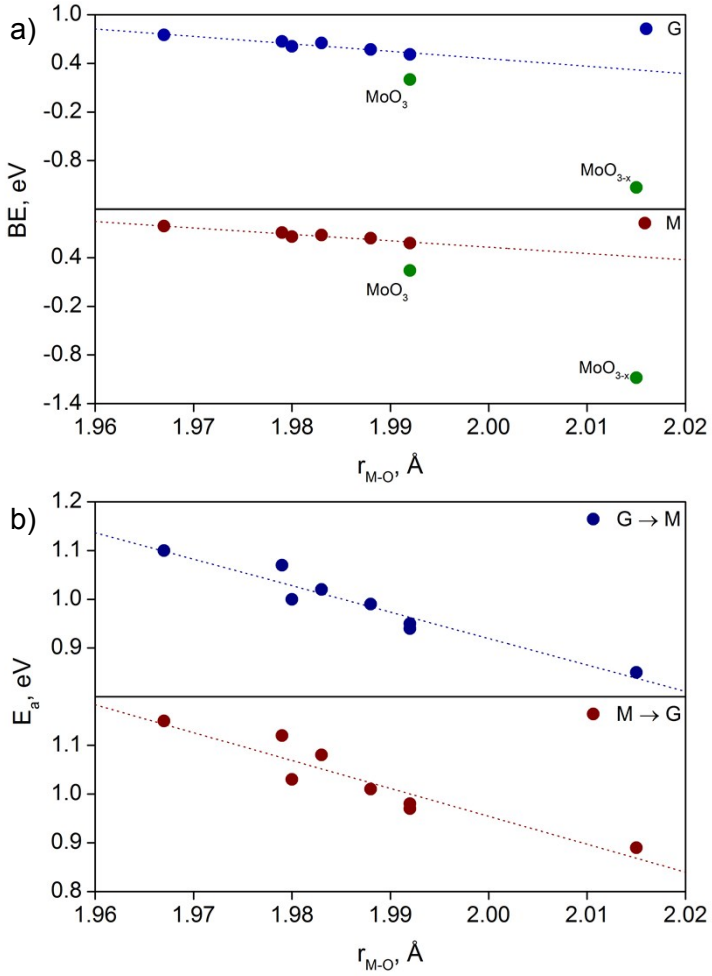

* The Mo-O bond distance is calculated by taking the average of the six Mo-O bonds. One of the oxygens is bounded to the heteroatom in POMs and it is a subsurface O in MoO_3. For MoO_{3-x}, Mo^{+5} centre, the four oxygens in the plane of the vacancy and a sublayer oxygen are considered.

Figure SI14. a) Reaction rate dependence of the temperature for a conversion of glucose to mannose of 0.01% on MoO_3, $H_nXMo_{12}O_{40}$ (X=S, P, As, Si, and Ge), and on $H_6P_2Mo_{18}O_{62}$. b) Apparent activation energy, E_{app}, for the different catalyst.

a)

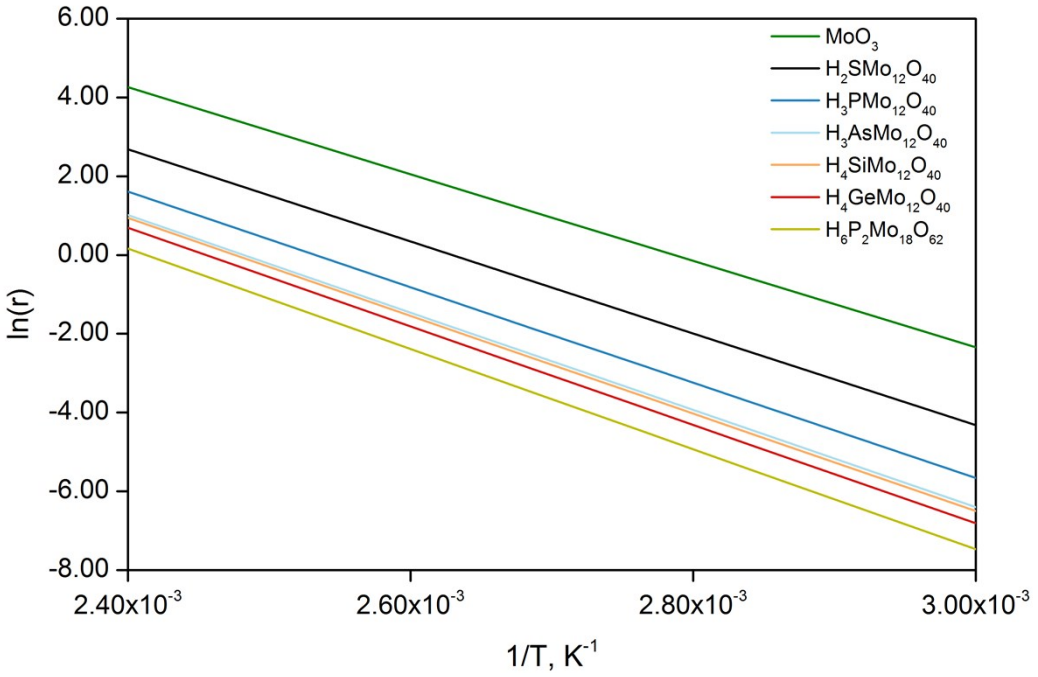

b)

Catalyst	Slope, K^{-1}	E_{app}, eV
MoO_3	-11012.70	0.95
$H_2SMo_{12}O_{40}$	-11672.69	1.00
$H_3PMo_{12}O_{40}$	-12119.29	1.04
$H_3AsMo_{12}O_{40}$	-12367.23	1.07
$H_4SiMo_{12}O_{40}$	-12399.16	1.07
$H_4GeMo_{12}O_{40}$	-12503.13	1.08
$H_6P_2Mo_{18}O_{62}$	-12722.66	1.10